DALTON

New atropisomeric bidentate nitrogen-donor compounds as potential stereocontrollers in mild CO–styrene copolymerisation catalysed by palladium(II) salts†

Barbara Milani,*[a] Enzo Alessio,[a] Giovanni Mestroni,[a] Ennio Zangrando,[a] Lucio Randaccio[a] and Giambattista Consiglio[b]

[a] *Dipartimento di Scienze Chimiche, Università di Trieste, Via L. Giorgieri 1, 34127 Trieste, Italy*
[b] *Eidgenössische Technische Hochschule, Laboratorium für Technische Chemie, ETH-Zentrum, Universitätstrasse 6, CH-8092 Zürich, Switzerland*

Two new atropisomeric bidentate nitrogen-donor chelating ligands, namely (−)-(*S*,*S*)-3,3′-(1,2-dimethylethylenedioxy)-2,2′-bipyridine L^1 and (+)-(*R*)-3,3′-(1-methylethylenedioxy)-2,2′-bipyridine L^2, have been synthesised and characterised. The crystal structure of L^2 confirmed its atropisomeric nature, the dihedral angle between the planes containing the pyridine rings being 50.1(1)°. The interaction of the new compounds, with palladium(II) salts led to the corresponding monochelated palladium complexes, $[PdL^1(O_2CCF_3)_2]$ **1** and $[PdL^2(O_2CCF_3)_2]$ **2**, the crystal structures of which have been determined. Both complexes crystallised with two independent molecules in the unit cell. In the two molecules of **1** the ligand L^1 is in the same conformation; while for **2** the two independent molecules correspond to two different atropisomers. The co-ordination geometry around palladium is square planar in all the molecules. In the two independent molecules of **1** and **2** the dihedral angle between the pyridine rings is considerably smaller than that observed in free L^2. The complexes are very active catalyst precursors in CO–styrene copolymerisation under mild reaction conditions (P_{CO} = 1 atm, 30 °C). The inhibiting role of carbon monoxide is evidenced. A low asymmetric induction was observed together with short isotactic sequences in the copolymer chain.

The last few years have witnessed increased industrial and academic interest in the carbon monoxide–olefin copolymerisation yielding perfectly alternating polyketones.[1–8] Among them, the polyketone with ethylene will be commercially exploited under the name of Carilon.[9] The reaction is homogeneously catalysed by palladium(II) compounds and two main approaches involving either *in situ* systems or presynthesised complexes have been applied. The *in situ* systems comprise $[Pd(O_2CMe)_2]$ or $[Pd(O_2CCF_3)_2]$ with a bidentate chelating phosphorus- or nitrogen-donor, a suitable acid as cocatalyst and, frequently, an oxidant such as benzoquinone.[1] The second approach involves presynthesised complexes, such as $[Pd(L\text{–}L)_2][PF_6]_2$,[3] $[Pd(L\text{–}L)(O_2CCF_3)_2]$[10] [L–L = 2,2′-bipyridine (bipy), 1,10-phenanthroline (phen) and their substituted derivatives] and the oxidant. In this case high yields can be obtained without any acid cocatalyst. Also organometallic compounds, such as $[Pd(L\text{–}L)Me(NCMe)][BR_4]$ (R = aryl),[11] are good catalyst precursors for the CO–olefin copolymerisation without any acid cocatalyst and any oxidant. In each case the reaction is preferentially run in methanol.

Particular attention has been devoted to the copolymerisation of CO with substituted olefins, such as propene[12] and styrene.[13–17] In this case the stereochemical control of the copolymer is a relevant goal. Good yields of the carbon monoxide–styrene copolymer can be obtained both with the *in situ* system $[Pd(O_2CMe)_2]$ + phen + *p*-$MeC_6H_4SO_3H$ + benzoquinone[17] and with the complex $[Pd(L\text{–}L)_2][PF_6]_2$ or $[Pd(L\text{–}L)(O_2CCF_3)_2]$ + benzoquinone.[10] The copolymer has a complete head-to-tail regioselectivity, which results from secondary insertions of styrene units,[17] and also a highly stereoregular structure, which has been identified as syndiotactic by the interpretation of the X-ray powder spectra[2] and ^{13}C NMR spectra.[18] According to studies on the stereospecific

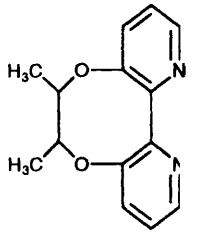

L^1

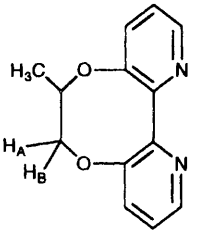

L^2

polymerisation of olefins, stereocontrol can arise from the last asymmetric carbon atom in the growing chain, or from the chiral environment of the metal atom or from both factors. The origin of stereoregularity may be different for isotactic and syndiotactic polymers.[19] Experimental evidence suggests that for the syndiotactic CO–styrene copolymer the stereochemistry is chain-end controlled.[17,18]

A forcing chiral environment on the metal atom might allow discrimination between the two faces of the prochiral olefin and lead to an isotactic copolymer. Our approach to the problem was based on the following facts: (*i*) 2,2′-bipyridine is the most active compound in the CO–styrene copolymerisation and (*ii*) owing to a twist about the C(2)–C(2′) axis, it is a potential source of conformational isomerism. The barrier to interconversion between the two atropisomers could be increased by bridging 2,2′-bipyridine at the 3,3′ positions.[20] Therefore, we synthesised two new atropisomeric bidentate nitrogen donors with the 2,2′-bipyridine skeleton, namely (−)-3,3′-(1,2-dimethylethylenedioxy)-2,2′-bipyridine (L^1) and (+)-3,3′-(1-methylethylenedioxy)-2-2′-bipyridine (L^2): the former has one C_2 symmetry axis and two chiral centres; the latter has no symmetry elements and one chiral centre. Both are atropisomeric and diastereomeric chelating.

In this paper we report the synthesis and the characterisation

† *Non-SI units employed:* bar = 10^5 Pa, atm = 101 325 Pa.

of the two new compounds, of the corresponding monochelated palladium(II) complexes, $[PdL^1(O_2CCF_3)_2]$ **1** and $[PdL^2(O_2CCF_3)_2]$ **2** and their catalytic activity in the CO–styrene copolymerisation. In the course of our work reports concerning the enantioselective isotactic alternating copolymerisation of styrene and 4-alkylstyrenes with carbon monoxide have appeared.[14,15]

Experimental

Starting materials

(2*R*,3*R*)-Butane-2,3-diol and (*S*)-propane-1,2-diol, organic reagents, palladium acetate and palladium trifluoroacetate were obtained from Aldrich and used as received. Analytical grade solvents (Baker) were used without further purification for synthetic and spectroscopic purposes. Methanol (Baker) for catalytic reactions was purified by distillation from magnesium and iodine and styrene was freshly distilled over $LiAlH_4$. Carbon monoxide (CP grade, 99.9%) was supplied by SIAD.

Physical measurements

Infrared spectra were recorded on a Perkin-Elmer 983G spectrometer as Nujol mulls between CsI plates for the new compounds and the complexes, in KBr pellets for the CO–styrene copolymer. Proton and ^{13}C NMR spectra were recorded at 400 and 100.5 MHz, respectively, on a JEOL EX 400 spectrometer operating in the Fourier-transform mode, with tetramethylsilane ($SiMe_4$) as internal standard. Two-dimensional nuclear Overhauser effect spectroscopy (NOESY) was done with a $\frac{\pi}{2}$ pulse of 12.6 μs. Two-dimensional homo- and hetero-nuclear correlated spectra were obtained with the automatic program of the instrument. The ^{13}C NMR spectra of the copolymer were recorded in $(CF_3)_2CHOH$ with a small amount of $CDCl_3$ for locking purposes and $SiMe_4$ as internal standard. Gas chromatographic analyses were carried out on a Hewlett-Packard 5890 II GC instrument with a flame ionisation detector and a 25 m (0.32 mm inside diameter) cross-linked methyl silicone capillary column. Optical rotations were determined with a Perkin Elmer 241 polarimeter.

Synthesis of compounds L^1 and L^2

Compounds L^1 and L^2 were synthesised by a procedure similar to that reported for analogous compounds (Scheme 1).[21] The di-*p*-tosylate derivatives **I** of the two diols were synthesised according to the described procedure.[22] (+)-3,3′-(1,2-dimethylethylenedioxy)bis(2-bromopyridine) and (−)-3,3′-(1-methylethylenedioxy)bis(2-bromopyridine) **II** were prepared as reported,[21] but with different ratios of the reagents, and in particular with 2-bromo-3-hydroxypyridine:di-*p*-tosylate **I** = 4:1 instead of 3:1 and sodium hydroxide:di-*p*-tosylate **I** = 8:1 instead of 6:1.

(+)-3,3′-(1,2-Dimethylethylenedioxy)bis(2-bromopyridine): yield 70%, α (589 nm, *c* 0.63 $CHCl_3$) = +50.27° (Found: C, 42.2; H, 3.55; Br, 39.10; N, 6.40. $C_{14}H_{14}Br_2N_2O_2$ requires C, 41.8; H, 3.50; Br, 39.75; N, 6.95%) $\delta_H(CDCl_3)$ 7.99 (2 H, m), 7.22 (4 H, m), 4.66 (2 H, m, CH) and 1.46 (6 H, d, Me).

(−)-3,3′-(1-Methylethylenedioxy)bis(2-bromopyridine): yield 80%, α (589 nm, *c* 0.65, $CHCl_3$) = −16.24° (Found: C, 40.40; H, 3.20; Br, 41.10; N, 7.20. $C_{13}H_{12}Br_2N_2O_2$ requires C, 40.25; H, 3.10; Br, 41.20; N, 7.20%); $\delta_H(CDCl_3)$ 8.03 (2 H, m), 7.45 (1 H, m), 7.20 (3 H, m), 4.86 (1 H, m, C*H*Me), 4.25 (2 H, m, CH_2), and 1.55 (3 H, d, Me).

A solution of $NiCl_2{\cdot}6H_2O$ (32.8 mmol) and triphenylphosphine (130.9 mmol) in dimethylformamide (dmf) (120 cm^3) was heated at 50 °C with efficient stirring under nitrogen. Zinc powder (32.8 mmol) was added to the blue solution which turned green and then red-brown. After 1 h the dibromide **II** (16.4 mmol) dissolved in dmf (45 cm^3) was added and the mixture stirred at 50 °C for 24 h. It was then poured into ammonium hydroxide (25%, 600 cm^3), extracted with chloroform, washed with water and dried (Na_2SO_4). The chloroform was rotoevaporated, and dimethylformamide distilled at reduced pressure. When the resulting brown oil was treated with methanol most of the triphenylphosphine precipitated. After filtration of phosphine and evaporation of methanol the yellow oil was purified by flash chromatography on silica gel (230–430 mesh). Elution with ethyl acetate–hexane (60:40) gave triphenylphosphine, with ethyl acetate–hexane (80:20) gave triphenylphosphine oxide and finally with ethyl acetate–ethanol (80:20) gave the product. This was obtained as a white solid.

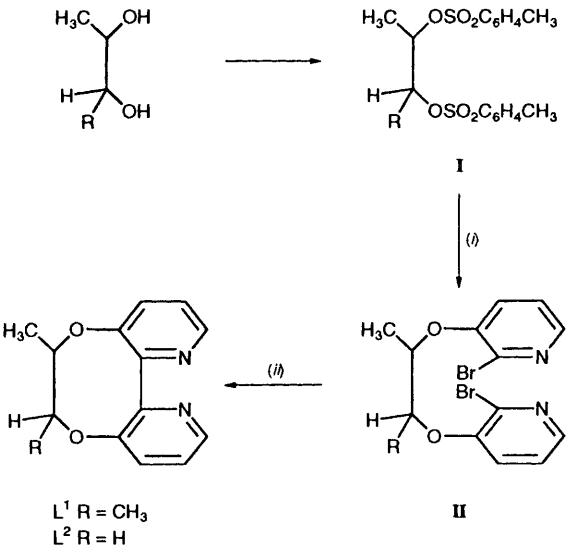

Scheme 1 (*i*) 2-Bromopyridin-3-ol, NaOH; (*ii*) $NiCl_2{\cdot}6H_2O$, PPh_3, Zn

(−)-(*S*,*S*)-3,3′-(1,2-Dimethylethylenedioxy)-2,2′-bipyridine: yield 35%, α (589 nm, *c* 0.69, $CHCl_3$) = −113.3° (Found: C, 68.4; H, 5.85; N, 10.80. $C_{14}H_{14}N_2O_2$ requires C, 69.4; H, 5.80; N, 11.55%); $\delta_H(CD_2Cl_2)$ 8.58 (2 H, dd, $H^{6,6'}$), 7.46 (2 H, dd, $H^{4,4'}$), 7.34 (2 H, dd, $H^{5,5'}$), 3.49 (2 H, m, CH), and 1.41 (6 H, dd, Me); $\delta_C(CD_2Cl_2$, 25 °C) 155 ($C^{2,2'}$), 149 ($C^{3,3'}$), 130 ($C^{4,4'}$), 125 ($C^{5,5'}$) 146 ($C^{6,6'}$), 85 (CH), and 19 (Me).

(+)-(*R*)-3,3′-(1-Methylethylenedioxy)-2,2′-bipyridine: yield 40%, α (589 nm, *c* 0.53, $CHCl_3$) = +138.03° (Found: C, 67.3; H, 5.20; N, 11.90. $C_{13}H_{12}N_2O_2$ requires C, 68.3; H, 5.30; N, 12.25%); $\delta_H(CD_2Cl_2)$ 8.52 (2 H, m, $H^{6,6'}$), 7.48 (2 H, m, $H^{4,4'}$), 7.36 (2 H, m, $H^{5,5'}$), 4.42 (1 H, br, CH_2), 3.80 (1 H, br, CH_2), 4.31 (1 H, br, CH), and 1.39 (3 H, d, Me); $^2J(CH_2)$ 12, $^3J(CH_2$–CH) 3, 10 at −40 °C in CD_2Cl_2; $^2J(CH_2)$ 12.5, $^3J(CH_2$–CH) 3.3, 10 Hz at +75 °C in $(CD_3)_2SO$; δ_C[$(CD_3)_2SO$, 75 °C] 155 ($C^{2,2'}$), 149 ($C^{3,3'}$), 130 ($C^{4,4'}$), 125 ($C^{5,5'}$), 145 ($C^{6,6'}$), 77 (CH_2), 80 (CH) and 17 (Me).

Synthesis of complexes 1 and 2

The complexes can be prepared either from $[Pd(L\text{–}L)(O_2CMe)_2]$ according to the procedure already reported for the corresponding achiral ligands[10] or from palladium acetate by following our new method (Scheme 2). The compound $[Pd(O_2CMe)_2]$ (4.4 mmol, 1 g) was dissolved at room temperature in methanol (90 cm^3). After 5 min the compound L–L (5.28 mmol, Pd:L–L = 1:1.2) was added as a solid to the stirred solution, which turned from red to yellow. The solution was then filtered over fine paper and an excess of CF_3CO_2H added (Pd:CF_3CO_2H = 1:27). In a few minutes the product precipitated as a yellow solid and after 30 min, it was filtered off, washed with cold methanol and vacuum dried.

$[PdL^1(O_2CCF_3)_2]$ **1**: yield 65%, α (589 nm, *c* 0.5274, $CHCl_3$) = +175.96° (Found: C, 37.2; H, 2.35; N, 4.70.

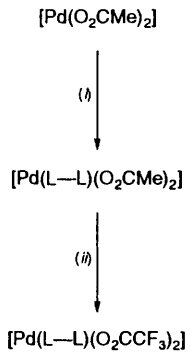

Scheme 2 L–L = L^1 or L^2. (*i*) L–L, MeOH; (*ii*) excess of CF_3CO_2H

$C_{18}H_{14}F_6N_2O_6Pd$ requires C, 37.6; H, 2.45; N, 4.85%); IR (cm^{-1}) $\nu_{asym}(CO_2)$ 1713, $\nu_{sym}(CO_2)$ 1403, $\Delta\nu$ = 310 (KBr pellets); $\delta_H(CD_2Cl_2)$ 8.00 (2 H, d, $H^{6,6'}$), 7.75 (2 H, dd, $H^{4,4'}$), 7.51 (2 H, m, $H^{5,5'}$), 4.44 (2 H, m, CH), and 1.33 (6 H, m, Me).

$[PdL^2(O_2CCF_3)_2]$ **2**: yield 70%, α (589 nm, *c* 0.5044, $CHCl_3$) = −71.57° (Found: C, 36.4; H, 2.10; N, 4.85. $C_{17}H_{12}F_6N_2O_6Pd$ requires C, 36.4; H, 2.15; N, 5.00%); IR (cm^{-1}) $\nu_{asym}(CO_2)$ 1717, $\nu_{sym}(CO_2)$ 1405, $\Delta\nu$ = 312 (KBr pellets); $\delta_H(CD_2Cl_2)$ 8.00 (2 H, m, $H^{6,6'}$), 7.87 (2 H, m, $H^{4,4'}$), 7.54 (2 H, m, $H^{5,5'}$), 4.60 (1 H, m, CH), 4.22 (2 H, m, CH_2), 1.44 (3 H, d, Me); $^2J(CH_2)$ 13, $^3J(CH_2$–CH) 3, 7 Hz.

Crystallography

Suitable crystals were obtained upon recrystallisation from hexane for compound L^2 and directly from the synthetic mixture (new method) for complexes **1** and **2**. Details of crystal parameters, data collection and refinements are summarised in Table 1. Unit-cell dimensions were previously determined by Weissenberg photographs, later refined by least-squares treatment of 25 reflections in the range θ 10–17° for all compounds. Diffraction data were collected at room temperature on an Enraf-Nonius CAD4 diffractometer equipped with a graphite monochromator and Mo-Kα radiation (λ = 0.7107 Å). The intensities of three reference reflections monitored during data collections did not show any decay for all compounds.

Reflections having intensities $I > 2\sigma(I)$ for compound L^2 and $I > 3\sigma(I)$ for **1** and **2** were corrected for Lorentz-polarisation factors and used in subsequent refinements. The quality of the crystals did not allow a sufficient number of reflections to be collected at high values. An absorption correction, based on an empirical ψ scan, was applied to **1** and **2**, but not to L^2.

The structure of compound L^2 was solved by direct methods, while the positions of Pd in **1** and **2** were determined by the conventional Patterson method. All remaining non-H atoms were located by standard Fourier techniques. The refinements were carried out by full-matrix anisotropic least-squares methods. All but a small amount of the total scattering density is pseudo-symmetrically related in complex **1**, but the chiral nature of the complex led to an unambiguous assignment of the space group *P*1. Hydrogen atoms at calculated positions (C–H 0.95 Å) were introduced in final cycles of refinement as a fixed contribution ($B = 1.3B_{eq}$ of their bonded atom). The final weighting schemes were $1/\sigma(F_o)^2$, unit, and $1/[\sigma(F_o)^2 + (0.02F_o)^2 + 1.0]$ for L^2, **1** and **2**, respectively.

The fluorine atoms in complexes **1** and **2** have considerable thermal motion (see ORTEP[23] drawings), but no attempt was made to resolve this disorder, splitting F atoms over two positions. The absolute structure was confirmed using the Flack χ parameter,[24] −0.02(3) and 0.08(14) for **1** and **2**, respectively. For L^2 the absolute configuration was derived from that of **2**.

Atomic scattering factors and anomalous dispersion parameters were taken from ref. 25. All calculations were carried out on a μ-VAX2000 computer using the Enraf-Nonius CAD4 system of programs[26] and the SHELXL 93 package.[27] Final atomic coordinates are reported in Tables 2–4.

Complete atomic coordinates, thermal parameters and bond lengths and angles have been deposited at the Cambridge Crystallographic Data Centre. See Instructions for Authors, *J. Chem. Soc., Dalton Trans.*, 1996, Issue 1.

Copolymerisation reactions

The copolymerisation reactions were carried out in a three-neck round-bottomed flask (100 cm^3) connected with a refrigerator, a thermometer and a carbon monoxide gas line. After introduction of the catalytic solution, comprising the solvent (methanol), catalyst precursor, quinone and styrene, carbon monoxide was continuously bubbled into the reaction mixture, heated with a thermostatted oil-bath to the reaction temperature. After 2 h the carbon monoxide flow was stopped and the mixture cooled to room temperature. Methanol (200 cm^3) was added and the copolymer filtered off, washed with methanol and vacuum dried at room temperature.

Carbonylation reactions

The carbonylation reactions were carried out in a stainless-steel autoclave (250 cm^3) containing $[Pd(O_2CCF_3)_2]$ (0.20 mmol), the atropisomeric compound (0.30 mmol), 1,4-benzoquinone (103.6 mmol), 1,4-hydroquinone (53.0 mmol), styrene (77.5 mmol) and methanol (100 cm^3). The autoclave was pressurised with 40 bar of CO and heated in an oil-bath at 70 °C for 48 h. After cooling and releasing the gas, the mixture was analysed by capillary gas chromatography. The extent of conversion of styrene was 76%. The product composition was: 1.3% methyl cinnamate, 38% dimethyl 2-phenylbutanedioate, *p*-hydroxyphenyl methyl 2-phenylbutanedioate (small amount), dimethyl 4-oxo-2,5-diphenylheptanedioate (small amount). The enantiomeric excess was determined by enantioselective capillary gas chromatography, using a Macherey-Nagel Lipodex E (50 m) column.

Results and Discussion

Synthesis and characterisation of compounds L^1 and L^2

The procedure for the synthesis of compounds L^1 and L^2 consists of the formation of the bis(2-bromopyridine) derivative followed by an intramolecular C–C coupling reaction (Scheme 1).[21] The main differences from the method previously reported[21] for a similar compound are in the second step. This is mediated by $[Ni(PPh_3)_4]$, prepared *in situ* through reduction of nickel(II) chloride by zinc powder. The reported procedure gave a low yield, presumably due to problems related with the purification of the final product from the great excess of phosphine. This is however, necessary to promote the intramolecular coupling of aryl halides.[28] We improved the yield of this step by treating the brown oil, resulting from the reaction mixture after evaporation of solvent, with methanol, in which the product is soluble, while most of the PPh_3 precipitates and can be easily separated.

Compound L^2 crystallises with two independent molecules in the unit cell. Fig. 1 depicts the ORTEP drawing with the atom numbering scheme for molecule A. The bond lengths and angles of the two molecules, which appear in the normal range, are equal within their estimated standard deviations (e.s.d.s). The conformations of the two molecules, (Fig. 2), which are similar, will be discussed later in connection with those in the palladium complexes. The dihedral angle between the planes containing the pyridine rings is 50.1(1) and 50.2(1)° in molecules A and B, respectively, confirming the atropisomeric structure of the

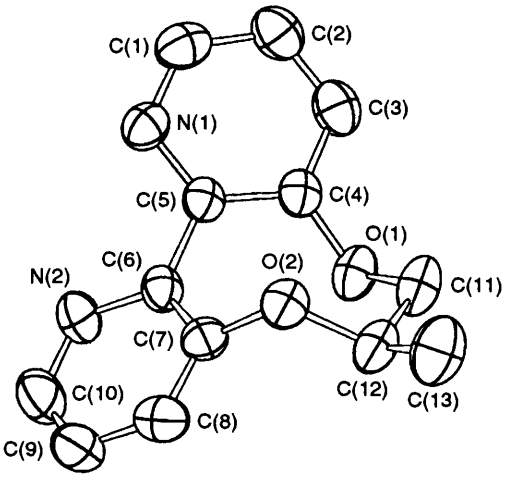

Fig. 1 An ORTEP drawing (50% probability thermal ellipsoids) of molecule A of compound L^2. The same labelling scheme applies also to molecule B

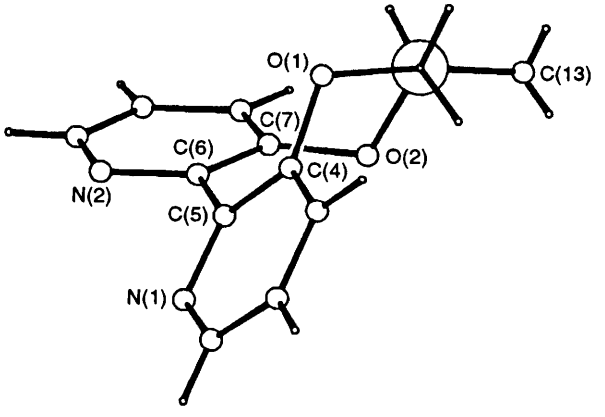

Fig. 2 Conformation of compound L^2 viewed along the C(11)–C(12) bond

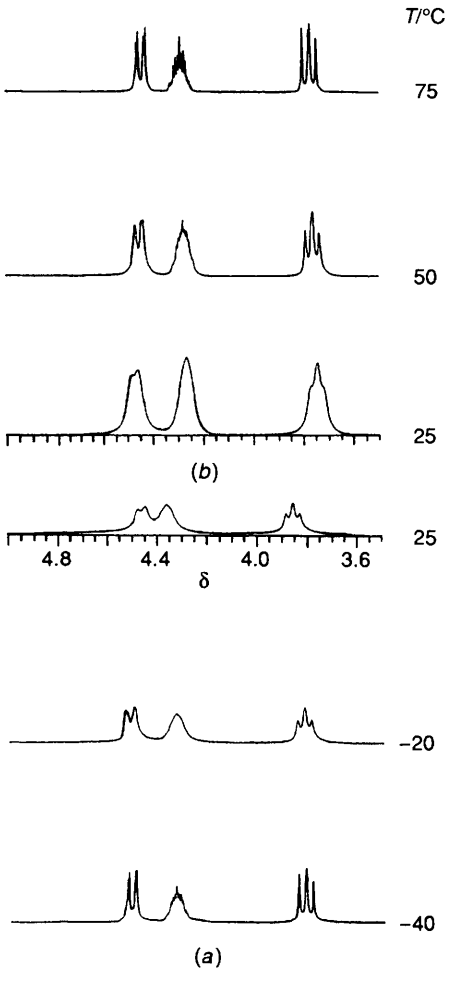

Fig. 3 Variation with temperature of the ^1H NMR spectra of compound L^2 (*a*) in CD_2Cl_2; (*b*) in $(CD_3)_2SO$

compound. The absolute configuration of the atropisomeric moiety can be assigned as *M* according to the rules of Cahn *et al.*[29] for the axial chirality. The absolute configuration of the chiral centre is *R*.

The characterisation in solutions of compounds L^1 and L^2 was done by NMR spectroscopy. Owing to the C_2 symmetry of the molecule, the NMR spectrum of L^1 is more straightforward and will be examined first. The aromatic region shows three very sharp double doublets, each integrating for two protons. The most downfield signal was assigned to the $H^{6,6'}$ protons, which lie closer to nitrogen. In a correlation (COSY) spectrum only the resonance centred at δ 7.34 shows cross-peaks with both the other signals, and can be therefore safely assigned to $H^{5,5'}$ protons. The groups of the bridge give sharp resonances of the expected multiplicity. Carbon signals were assigned by means of heterocorrelated ^1H–^{13}C and proton-coupled NMR spectra.

The aromatic region of compound L^2 is characterised by three multiplets, each integrating for two protons, but their fine structure is more complicated than that of L^1. Each multiplet is very likely due to the overlap of the two resonances of like protons on the two non-equivalent aromatic rings. They were assigned as above even though a distinction between the two rings was not attempted. The resonances of the two diastereotopic methylenic protons of the bridge were unambiguously distinguished from the resonance of the methyne proton with a heterocorrelated ^1H–^{13}C NMR spectrum. The multiplets of the methylene protons, in fact, are related to the same carbon atom. This spectrum also allowed us to assign most of the ^{13}C signals. The signals of the quaternary carbon atoms of the pyridine rings ($C^{3,3'}$ and $C^{2,2'}$) were assigned on the basis of the proton-coupled ^{13}C NMR spectrum, $C^{3,3'}$ being split into a doublet by long-range coupling with $H^{4,4'}$, while $C^{2,2'}$ remains a singlet.

While for compound L^1 all the proton signals are sharp at room temperature, in the case of L^2 the resonances of the bridge protons are rather broad [CD_2Cl_2, $(CD_3)_2SO$)], implying conformational mobility. The three signals become better resolved both upon decreasing the temperature [in CD_2Cl_2, Fig. 3(*a*)] and upon raising it [in $(CD_3)_2SO$, Fig. 3(*b*)].

For similar bridged bipyridine systems rotation about the 2,2′ bond to relieve the torsional strain in the annelated bridge and a certain rigidity had been proposed.[12] The two limiting conformations obtained upon twisting the 2,2′ bond would be diastereomeric for our compounds. We interpret the NMR behaviour of L^2 with temperature as showing the presence of a largely prevailing conformer. Furthermore, this must be true also for L^1. Since rigidity is increased by increasing substitution on the bridge,[22] its conformational equilibrium is fixed at room temperature. The coupling pattern observed for L^2 strongly infers a conformation similar to that observed in the solid state.

Synthesis and characterisation of complexes 1 and 2

The complexes $[PdL^1(O_2CCF_3)_2]$ **1** and $[PdL^2(O_2CCF_3)_2]$ **2** can be synthesised according to the procedure reported for the corresponding achiral complexes, $[Pd(L–L)(O_2CCF_3)_2]$,[10] or by following an easier procedure which avoids isolation of the acetato derivatives. Dissolution of $[Pd(O_2CMe)_2]$ in methanol, followed by addition of the compound L–L (L^1 or L^2) as a solid yields a yellow solution of $[Pd(L–L)(O_2CMe)_2]$, from which

the product precipitates upon addition of an excess of trifluoroacetic acid (Scheme 2). By this procedure the complexes can be obtained in high yield and do not require any recrystallisation.

The separation between the symmetric and asymmetric carboxylato carbon–oxygen stretching bands $\Delta\nu$ is diagnostic of the binding mode of the ligand.[30] In complexes **1** and **2** $\Delta\nu$ is considerably larger than for the free carboxylate anion, suggesting a unidentate (end-on) co-ordination of trifluoroacetate. This is in agreement with our previous studies on the corresponding achiral derivatives.[10]

Two crystallographically independent molecules were detected in the unit cells of complexes **1** and **2**. Figs. 4 and 5 show ORTEP drawings of one molecule of **1** and both molecules of **2**, respectively, while selected bond lengths and angles are reported in Table 5. The Pd–N distances in both complexes are equal within their e.s.d.s. These distances are comparable with those found in $[Pd(bipy)L_2]$ complexes (L = O-donor ligands)[31] and in $[Pd(phen)(O_2CMe)_2]$.[10] The trifluoroacetate ligands are confirmed to assume a unidentate end-on co-ordination, oriented on the same side of the co-ordination plane. The co-ordination about Pd is square planar. In complex **1** the metal lies in the O_2N_2 co-ordination mean plane in molecule A, while a displacement of 0.38 Å is detected in molecule B. The Pd in complex **2** lies 0.044 Å out of the plane in molecule A and 0.005 Å in B.

Table 6 reports some geometrical parameters defining the conformations of the free compound L^2 and of co-ordinated L^1 and L^2 in complexes **1** and **2** respectively. In the two crystallographically independent molecules of **1** and **2** the dihedral angle between the pyridine rings falls in the range 14–21°, considerably reduced with respect to that of *ca.* 50° observed in free L^2. This allows a suitable co-ordination to the metal, in other words the chelation of the ligand forces the two rings towards planarity. The two molecules of **1** are arranged head-to-tail with an unusually short Pd···Pd distance of 3.2536(4) Å between them. They are conformationally very similar (Fig. 4), the absolute configuration of the atropisomeric moiety being *M*.[29] In **2** the two independent molecules are different as evidenced from Fig. 5. They correspond to two different atropisomers (*M* for A and *P* for B), as also appears from the opposite sign of the torsional angle N(1)–C(5)–C(6)–N(2) (Table 6).

Fig. 6 gives a perspective view of the co-ordinated N-donor ligand in complexes **1** and **2** along the C(11)–C(12) bond. The methyl groups C(13) and C(14) are in *anti* position with respect to the oxygens in the two molecules of **1** [Fig. 6(*a*)], as well as for molecule B of **2** [Fig. 6(*c*)]. On the other hand, molecule A in **2** is a different conformer with the methyl group *gauche* to O(1) [Fig. 6(*b*)]. Figs. 2 and 6 display the different arrangements of oxygens in free L and in the complexes, being on the opposite sides of an ideal plane C(11), C(12), C(5), C(6) in the former and on the same side in the complexes. Although this comparison shows the great flexibility of the ligand, the co-ordination to Pd might induce a strain in the propane- and butane-dioloxy bridges, as appears from the increased bond angles at oxygens (up to 123°), compared with the value observed in free L^2 (Table 6).

The behaviour in solution of both complexes was studied by ^1H NMR spectroscopy in CD_2Cl_2. The aromatic signals are shifted downfield relative to free L^2 or L^1, except those due to $H^{6,6'}$, which are shifted upfield (about 0.50–0.60 ppm). This is in agreement with our previous study of the achiral trifluoroacetato derivatives.[10] The fine structure of the aromatic resonances is similar to that found for free L^1 or L^2. In the case of **2** the signals of the two diastereotopic protons gave a pattern typical of an ABX system. The coupling constants are very similar to those observed for free L^2. The NOESY spectrum of **2** presents a cross-peak between the signal of $H^{4,4'}$ and that of the methyne proton of the bridge and also that of

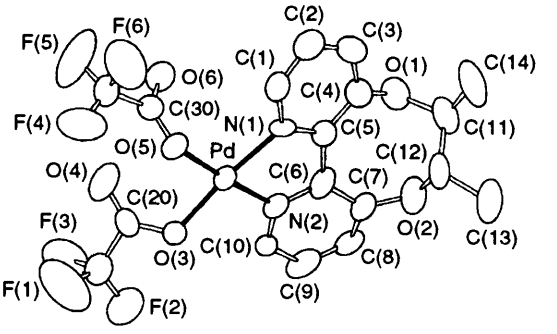

Fig. 4 An ORTEP drawing (50% probability thermal ellipsoids) and the labelling scheme of molecule A of complex **1**

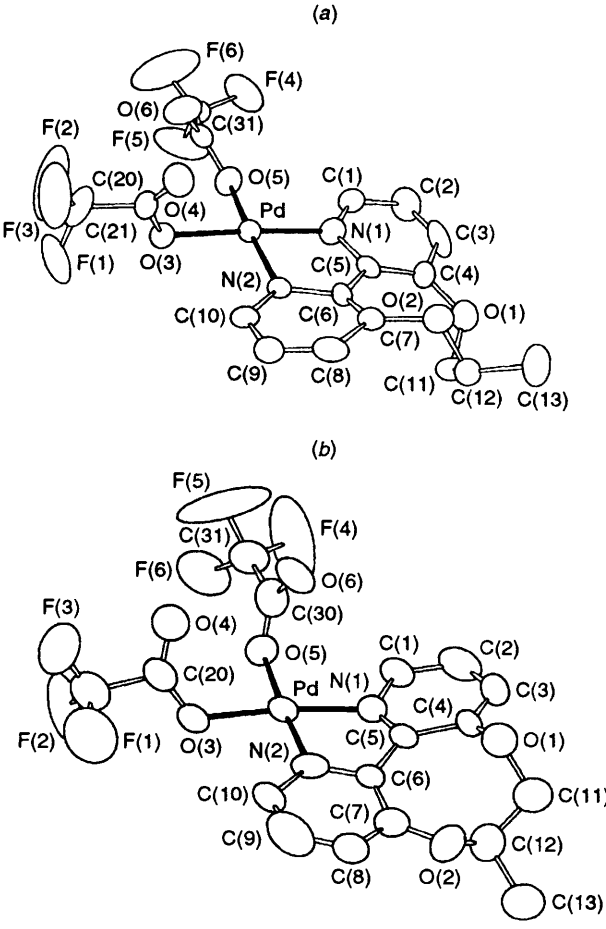

Fig. 5 An ORTEP drawing (50% probability thermal ellipsoids) and the labelling scheme of (*a*) molecule A and (*b*) molecule B of complex **2**

the methyl. This suggests that among the different conformers present in solution, one is similar to molecule A [Fig. 5(*a*)], where the non-bonding distances H(C8)···H(C12) and H(C8)···H(C13) are shorter than 5 Å. In fact the lines in the ^1H NMR spectrum in CD_2Cl_2 become broader on lowering the temperature and remain broad up to −90 °C.

For both complexes all the signals are sharp in CD_2Cl_2, while in $(CD_3)_2SO$ the resonances in the aromatic region and those of the bridge are broad and become better resolved upon addition of $Na(O_2CCF_3)$. This behaviour reveals the establishment of an equilibrium involving the dissociation of $CF_3CO_2^-$.[10]

Copolymerisation reactions

The effect of the two new atropisomeric chelating compounds on the CO–styrene copolymerisation and, in particular, on the stereochemistry of the CO–styrene copolymer was investigated. The catalytic system was first optimised with respect to pressure

Table 1 Crystallographic data and details of refinements for compound L^2 and complexes **1** and **2**

	L^2	**1**	**2**
Formula	$C_{13}H_{12}N_2O_2$	$C_{18}H_{14}F_6N_2O_6Pd$	$C_{17}H_{12}F_6N_2O_6Pd$
M	228.25	574.71	560.69
Crystal size/mm	0.4 × 0.4 × 0.15	0.2 × 0.2 × 0.6	0.3 × 0.2 × 0.7
Crystal system	Monoclinic	Triclinic	Monoclinic
Space group	$P2_1$ (no. 4)	$P\bar{1}$ (no. 1)	$P2_1$ (no. 4)
a/Å	10.827(5)	9.036(3)	13.205(7)
b/Å	8.918(5)	9.804(3)	9.233(3)
c/Å	12.847(7)	12.857(4)	17.237(7)
α/°		68.86(3)	
β/°	107.62(5)	88.78(2)	111.67(2)
γ/°		74.10(2)	
U/Å^3	1182.2(7)	1017.9(6)	1953(1)
D_c/g cm^{-3}	1.28	1.87	1.91
Z	4	2	4
μ(Mo-Kα)/cm^{-1}	0.8	9.9	10.3
F(000)	480	568	1104
$2\theta_{max}$/°	54	60	60
No. data measured	2879	6148	4812
Maximum, minimum transmission (%)	—	99.9, 93.3	99.8, 84.6
No. unique data	1882 [$I \geqslant 2\sigma(I)$]	5059 [$I \geqslant 3\sigma(I)$]	3638 [$I \geqslant 3\sigma(I)$]
No. parameters	307	593	577
R	0.059	0.034	0.049
R'	0.055	0.034	0.053
Goodness of fit*	1.72	1.05	1.21
Residuals/e Å^{-3}	0.25, −0.14	0.51, −0.12	0.73, −0.22

* Defined as $[(\Sigma w|F_o| - |F_c|^2)/(n - m)]^{\frac{1}{2}}$ where n = number of reflections and m = number of variables.

Table 2 Fractional atomic coordinates and their e.s.d.s for compound L^2

	Molecule A			Molecule B		
Atom	x	y	z	x	y	z
O(1)	0.2656(2)	0	0.2399(2)	0.6903(2)	0.5998(3)	0.1934(2)
O(2)	0.0168(2)	0.0767(3)	0.1198(2)	0.5863(2)	0.6297(3)	0.3647(2)
N(1)	0.0553(2)	−0.2565(3)	0.3237(2)	0.3604(3)	0.4613(3)	0.0926(2)
N(2)	0.0105(3)	0.0357(4)	0.3993(2)	0.4993(3)	0.2562(3)	0.2572(2)
C(1)	0.1108(4)	−0.3853(4)	0.3112(3)	0.3205(3)	0.5376(5)	0.0008(3)
C(2)	0.2149(3)	−0.3972(5)	0.2715(3)	0.3945(4)	0.6394(5)	−0.0326(3)
C(3)	0.2659(3)	−0.2688(5)	0.2447(3)	0.5189(4)	0.6630(5)	0.0312(3)
C(4)	0.2102(3)	−0.1331(4)	0.2566(2)	0.5635(3)	0.5878(4)	0.1301(2)
C(5)	0.1027(3)	−0.1310(4)	0.2949(2)	0.4815(3)	0.4882(4)	0.1585(2)
C(6)	0.0359(3)	0.0115(4)	0.3039(2)	0.5215(3)	0.4042(4)	0.2632(2)
C(7)	−0.0025(3)	0.1111(4)	0.2181(2)	0.5752(3)	0.4758(4)	0.3622(2)
C(8)	−0.0690(4)	0.2384(4)	0.2283(3)	0.6074(4)	0.3940(5)	0.4568(3)
C(9)	−0.0950(4)	0.2638(5)	0.3245(3)	0.5863(4)	0.2402(5)	0.4498(3)
C(10)	−0.0521(4)	0.1622(5)	0.4062(3)	0.5317(4)	0.1813(5)	0.3499(3)
C(11)	0.2387(3)	0.0457(4)	0.1287(2)	0.7197(4)	0.7286(5)	0.2646(4)
C(12)	0.1258(3)	0.1511(4)	0.0962(2)	0.7152(3)	0.6877(5)	0.3757(3)
C(13)	0.0865(4)	0.1844(6)	−0.0243(3)	0.7416(5)	0.8180(6)	0.4546(4)

and temperature using $[Pd(bipy)(O_2CCF_3)_2]$ as catalyst precursor, *i.e.* the achiral complex most similar to **1** and **2**. The catalytic activity at 1 atm, under a stream of CO, was twice that at 40 atm (Table 7). This result represents one of the first examples of copolymerisation at low pressure of carbon monoxide giving a high yield of copolymer. Moreover, it suggests the inhibiting role of carbon monoxide.

At low pressure the reaction can be carried out in a glass reactor, instead of a steel bomb, allowing observation of colour changes. At $T \geqslant 40$ °C the final product is grey, very likely due to the presence of palladium metal. At 30 °C the catalytic activity is higher than at 50 °C and no decomposition of the active species to palladium metal was observed, a clear white copolymer being obtained (Table 7). According to these results, $[Pd(bipy)(O_2CCF_3)_2]$ is one of the most active catalyst precursors among those operating under such mild conditions.[14,16]

The complexes with the atropisomeric ligands were tested under the same conditions. The catalytic activity is similar to that of $[Pd(bipy)(O_2CCF_3)_2]$ (Table 8), and the copolymer is optically active. The low optical activity could be related with the presence of the short isotactic sequences in the copolymer chain. The stereochemistry of the copolymer can be recognised by analysing the region due to the *ipso*-carbon atom in the decoupled ^{13}C NMR spectrum.[18] This region presents four signals, which can be attributed to the syndiotactic triad *rr* (the main one), to the two different atactic triads *rm* and *mr* and to the isotactic triad *mm* (Fig. 7). The intensity of the latter signal is about 10% of the sum of the intensities of the four signals. The signal of the isotactic triad is absent from the spectrum of the copolymer obtained with the achiral ligands.[18]

Complex **1** yielded a higher optical activity, and a higher content of isotacticity of the copolymer, compared to **2**. This might be correlated with the C_2 symmetry of L^1. Using a supporting ligand with a C_2 symmetry axis, Brookhart *et al.*[14] obtained completely isotactic CO–4-*tert*-butylstyrene. An isotactic CO–styrene copolymer has very recently been obtained, even though with very low catalytic activity, with a C_2 symmetry bioxazoline, as ancillary ligand.[16]

A low enantioface discriminating ability of complexes **1** and **2** was also recognised in the carbonylation of styrene in the

Table 3 Fractional atomic coordinates and their e.s.d.s for complex **1**

	Molecule A			Molecule B		
Atom	*x*	*y*	*z*	*x*	*y*	*z*
Pd	0	0	0	−0.342 19(5)	−0.790 05(5)	−0.119 06(4)
F(1)	−0.162 0(8)	−0.028(1)	0.381 5(6)	−0.160 9(6)	−0.360 1(6)	−0.185 3(5)
F(2)	−0.057(1)	0.139 4(6)	0.301 6(5)	−0.149 8(6)	−0.394 7(6)	−0.336 2(4)
F(3)	0.057 9(8)	−0.077 6(7)	0.416 3(4)	−0.338 2(6)	−0.221 1(4)	−0.308 7(4)
F(4)	−0.184 6(7)	−0.396 4(6)	0.203 0(6)	−0.134 4(7)	−0.849 4(9)	−0.441 8(5)
F(5)	−0.000 0(8)	−0.553 3(7)	0.208 1(7)	−0.322(1)	−0.908 8(7)	−0.438 7(6)
F(6)	−0.146 9(7)	−0.463 8(5)	0.070 8(5)	−0.322(1)	−0.706 2(9)	−0.542 7(5)
O(1)	0.331 7(5)	0.121 7(6)	−0.336 9(4)	−0.663 4(5)	−1.085 5(5)	0.169 5(4)
O(2)	0.226 0(6)	0.392 8(6)	−0.316 8(5)	−0.512 8(7)	−0.993 0(5)	0.293 9(4)
O(3)	−0.052 1(5)	0.042 9(4)	0.137 3(3)	−0.253 8(5)	−0.609 7(5)	−0.174 7(4)
O(4)	0.033 8(9)	−0.199 7(6)	0.263 7(5)	−0.478 3(5)	−0.427 8(5)	−0.207 3(5)
O(5)	−0.098 3(4)	−0.172 4(4)	0.051 5(3)	−0.283 9(5)	−0.830 7(4)	−0.262 3(4)
O(6)	0.131 6(5)	−0.349 8(5)	0.083 4(4)	−0.413 4(6)	−0.607 6(5)	−0.385 8(4)
N(1)	0.062 3(5)	−0.015 0(4)	−0.145 4(4)	−0.422 7(5)	−0.968 4(4)	−0.056 0(3)
N(2)	0.103 5(5)	0.166 6(5)	−0.055 3(4)	−0.397 3(5)	−0.770 1(6)	0.026 9(4)
C(1)	0.041 9(7)	−0.126 7(6)	−0.175 4(5)	−0.433 5(7)	−1.055 8(6)	−0.116 1(5)
C(2)	0.116(1)	−0.167 8(7)	−0.256 5(6)	−0.514 2(7)	−1.162 8(6)	−0.076 7(5)
C(3)	0.211(1)	−0.073 5(8)	−0.315 8(5)	−0.586 3(7)	−1.180 4(7)	0.021 4(6)
C(4)	0.225 5(7)	0.046 4(7)	−0.289 5(5)	−0.574 8(6)	−1.085 2(5)	0.081 4(4)
C(5)	0.145 2(6)	0.078 5(6)	−0.204 4(5)	−0.490 0(6)	−0.986 2(5)	0.043 9(4)
C(6)	0.143 5(6)	0.195 7(6)	−0.160 7(6)	−0.454 2(6)	−0.882 2(5)	0.096 9(4)
C(7)	0.199 5(7)	0.330 1(7)	−0.210 2(6)	−0.482 2(8)	−0.884 5(7)	0.204 6(5)
C(8)	0.231 8(6)	0.396 8(5)	−0.142 0(6)	−0.470(1)	−0.760 1(8)	0.229 3(5)
C(9)	0.189 0(7)	0.365 4(6)	−0.039 8(7)	−0.424(1)	−0.654 6(7)	0.159 2(5)
C(10)	0.114 6(7)	0.248 6(6)	0.001 3(5)	−0.381(1)	−0.655 1(7)	0.053 3(6)
C(11)	0.274 5(8)	0.258 1(9)	−0.437 8(6)	−0.595 6(7)	−1.196 2(7)	0.279 4(5)
C(12)	0.151 6(9)	0.372 5(9)	−0.411 0(6)	−0.462(1)	−1.154 3(8)	0.304 1(7)
C(13)	0.106(1)	0.529(1)	−0.502 1(8)	−0.563 8(9)	−1.358 7(8)	0.288 8(7)
C(14)	0.225(1)	0.223(1)	−0.534 3(6)	−0.396(1)	−1.239(1)	0.429 1(8)
C(20)	−0.013 5(8)	−0.063 0(7)	0.237 5(5)	−0.341 7(6)	−0.474 1(5)	−0.207 3(5)
C(21)	−0.031(1)	0.001 4(9)	0.332 2(7)	−0.246 5(9)	−0.361 7(7)	−0.257 9(6)
C(30)	−0.006 6(7)	−0.302 8(6)	0.093 6(5)	−0.327 9(7)	−0.733 9(6)	−0.356 0(5)
C(31)	−0.088 8(7)	−0.428 4(7)	0.148 5(5)	−0.267 0(8)	−0.795 6(8)	−0.446 7(5)

Table 4 Fractional atomic coordinates and their e.s.d.s for complex **2**

	Molecule A			Molecule B		
Atom	*x*	*y*	*z*	*x*	*y*	*z*
Pd	0.442 63(6)	0.5	0.305 63(4)	0.541 24(6)	0.250 6(1)	0.190 54(4)
F(1)	0.299 8(9)	0.192(1)	0.447 4(6)	0.830(1)	−0.001(2)	0.381 7(6)
F(2)	0.203 9(9)	0.329(3)	0.428 5(8)	0.914 7(7)	0.172(1)	0.368 3(7)
F(3)	0.310 9(9)	0.327(2)	0.535 3(5)	0.925 9(7)	−0.017(1)	0.309 9(7)
F(4)	0.159 9(9)	0.789(1)	0.125 9(6)	0.644 7(9)	0.510(1)	−0.011 5(7)
F(5)	0.102(1)	0.580(1)	0.109 0(6)	0.759 6(9)	0.348(2)	0.008 1(6)
F(6)	0.052(1)	0.718(2)	0.181 0(7)	0.781 5(7)	0.490(2)	0.097 2(5)
O(1)	0.810 3(7)	0.630(1)	0.267 4(5)	0.132 4(6)	0.154(1)	0.050 0(5)
O(2)	0.860 8(6)	0.590(1)	0.432 4(5)	0.164 5(6)	0.099(1)	0.210 2(5)
O(3)	0.355 5(5)	0.371 4(9)	0.353 7(4)	0.683 0(6)	0.172(1)	0.275 6(4)
O(4)	0.410 7(6)	0.512(1)	0.468 7(4)	0.758 9(7)	0.089(1)	0.187 6(5)
O(5)	0.300 4(6)	0.571(1)	0.221 3(5)	0.625 2(5)	0.375 3(9)	0.138 8(4)
O(6)	0.224 2(8)	0.653(1)	0.308 2(5)	0.583 4(7)	0.229(1)	0.030 2(4)
N(1)	0.533 5(7)	0.617(1)	0.259 9(5)	0.394 7(6)	0.318(1)	0.116 1(5)
N(2)	0.588 8(6)	0.433(1)	0.379 2(4)	0.449 0(7)	0.129 4(9)	0.234 4(5)
C(1)	0.490 6(9)	0.710(1)	0.197 2(6)	0.382 0(9)	0.412(1)	0.053 0(6)
C(2)	0.556(1)	0.784(2)	0.163 4(6)	0.279(1)	0.434(2)	−0.008 6(7)
C(3)	0.656(1)	0.757(2)	0.188 9(6)	0.192 0(8)	0.345(2)	−0.006 5(7)
C(4)	0.705 8(8)	0.658(1)	0.254 4(6)	0.208 3(7)	0.255(1)	0.054 1(5)
C(5)	0.641 6(8)	0.595(1)	0.294 9(6)	0.314 6(7)	0.238(1)	0.122 7(5)
C(6)	0.676 5(7)	0.505(1)	0.371 0(5)	0.340 5(7)	0.148(1)	0.196 5(5)
C(7)	0.771 6(7)	0.501(1)	0.429 3(6)	0.271 3(8)	0.084(1)	0.232 7(6)
C(8)	0.787(1)	0.397(1)	0.500 9(7)	0.316 7(8)	−0.012(2)	0.297 2(6)
C(9)	0.708 7(9)	0.316(1)	0.500 7(6)	0.427(1)	−0.032(2)	0.330 6(8)
C(10)	0.609 8(9)	0.337(1)	0.441 6(6)	0.493 3(9)	0.048(2)	0.304 8(6)
C(11)	0.861 4(9)	0.505(2)	0.302 9(7)	0.054 2(9)	0.209(2)	0.083 6(8)
C(12)	0.928 4(9)	0.526(2)	0.392 0(9)	0.113 3(9)	0.232(2)	0.174 0(8)
C(13)	1.017(1)	0.629(2)	0.405(1)	0.026(1)	0.263(3)	0.210 7(9)
C(20)	0.358 1(8)	0.417(1)	0.426 7(7)	0.753 8(9)	0.111(2)	0.254 5(7)
C(21)	0.296 1(9)	0.328(2)	0.465 2(7)	0.861(1)	0.061(2)	0.331 2(8)
C(30)	0.226 7(9)	0.628(1)	0.240 8(6)	0.627 7(8)	0.330(1)	0.072 3(5)
C(31)	0.136(1)	0.673(2)	0.165 9(9)	0.701(1)	0.429(2)	0.043 7(7)

Table 5 Selected bond lengths (Å) and angles (°) of complexes **1** and **2**

	1		**2**	
	Molecule A	B	Molecule A	B
Pd–O(3)	1.976(5)	2.028(5)	2.031(8)	2.038(6)
Pd–O(5)	2.019(4)	2.050(5)	2.013(7)	2.020(8)
Pd–N(1)	1.986(5)	1.973(4)	1.98(1)	1.986(7)
Pd–N(2)	2.005(5)	1.995(6)	1.977(7)	1.997(9)
O(3)–Pd–O(5)	90.3(2)	88.8(2)	88.1(3)	90.7(3)
O(3)–Pd–N(1)	171.5(2)	176.6(2)	176.9(4)	173.4(4)
O(3)–Pd–N(2)	92.0(2)	95.8(2)	97.0(3)	93.2(3)
O(5)–Pd–N(1)	98.1(2)	93.8(2)	94.4(4)	95.6(3)
O(5)–Pd–N(2)	177.4(2)	174.9(2)	173.9(4)	175.9(3)
N(1)–Pd–N(2)	79.4(2)	81.5(2)	80.4(3)	80.5(3)

Numbers in parentheses are e.s.d.s in the least significant digits.

Table 6 Geometrical parameters defining the conformations of compound L^2 and of L^1 and L^2 in **1** and **2***

	L^2	**1**	**2**
N(1)–C(5)–C(6)–N(2)	48.7(4)	18.9(7)	15(1)
	48.6(4)	14.6(7)	−18(1)
O(1)–C(11)–C(12)–O(2)	−55.0(3)	54.8(8)	53(1)
	−58.2(4)	55.0(7)	−56(1)
O(1)–C(11)–C(12)–C(13)	−172.9(3)	168.3(8)	−63(2)
	−178.4(3)	167.8(7)	−170(1)
C(14)–C(11)–C(12)–O(2)	—	−178.3(6)	—
	—	−178.7(6)	—
C(14)–C(11)–C(12)–C(13)	—	−65(1)	—
	—	−65.9(9)	—
py/py plane	50.1(1)	20.8(5)	206(8)
	50.2(1)	14.7(7)	16(1)
C(4)–O(1)–C(11)	115.8(2)	115.7(5)	123(1)
	115.3(3)	116.7(4)	111(1)
C(7)–O(2)–C(12)	116.4(2)	123.3(6)	113.4(9)
	115.5(3)	120.3(6)	120(1)

* Second value is for molecule B.

Table 7 Effect of carbon monoxide pressure and temperature on the carbon monoxide–styrene copolymerisation. Catalyst precursor [Pd(bipy)$(O_2CCF_3)_2$]

P_{CO}/atm	T/°C	g Copolymer per g Pd	g Copolymer per g Pd per h	t/h
40	50	207 (g)	34.5	6
1	50	175 (g)	87.5	2
1	40	122 (g)	61.0	2
1	30	282 (w)	141.0	2

Reaction conditions: n_{Pd} = 0.05 mmol, $n_{quinone}$ = 1 mmol, 10 cm^3 styrene, 20 cm^3 methanol. g = Grey, w = white.

Table 8 Effect of catalyst precursor on the carbon monoxide–styrene copolymerisation

Precursor	g Copolymer per g Pd	α (589 nm, 25 °C)[a]/°
[Pd(bipy)$(O_2CCF_3)_2$]	282	0
[$PdL^2(O_2CCF_3)_2$]	235	+4
[$PdL^1(O_2CCF_3)_2$]	260	−36

Reaction conditions: [Pd] = 1.7 × 10^{-3}, [1,4-benzoquinune] = 3.3 × 10^{-2} mol dm^{-3}; 10 cm^3 styrene, 20 cm^3 methanol; P_{CO} = 1 atm; 30 °C; 2 h. [a] Specific rotation [c 0.57, $(CF_3)_2CHOH$].

presence of an excess benzoquinone of (molar ratio benzoquinone: styrene about 1.3:1). Under these conditions dimethyl phenylsuccinate is predominantly formed, as expected.[32] The optical yield of the prevailing enantiomer (*ul* relative absolute configuration with respect to the ligand used) was 9.3 and 3.6 for **1** and **2**, respectively.

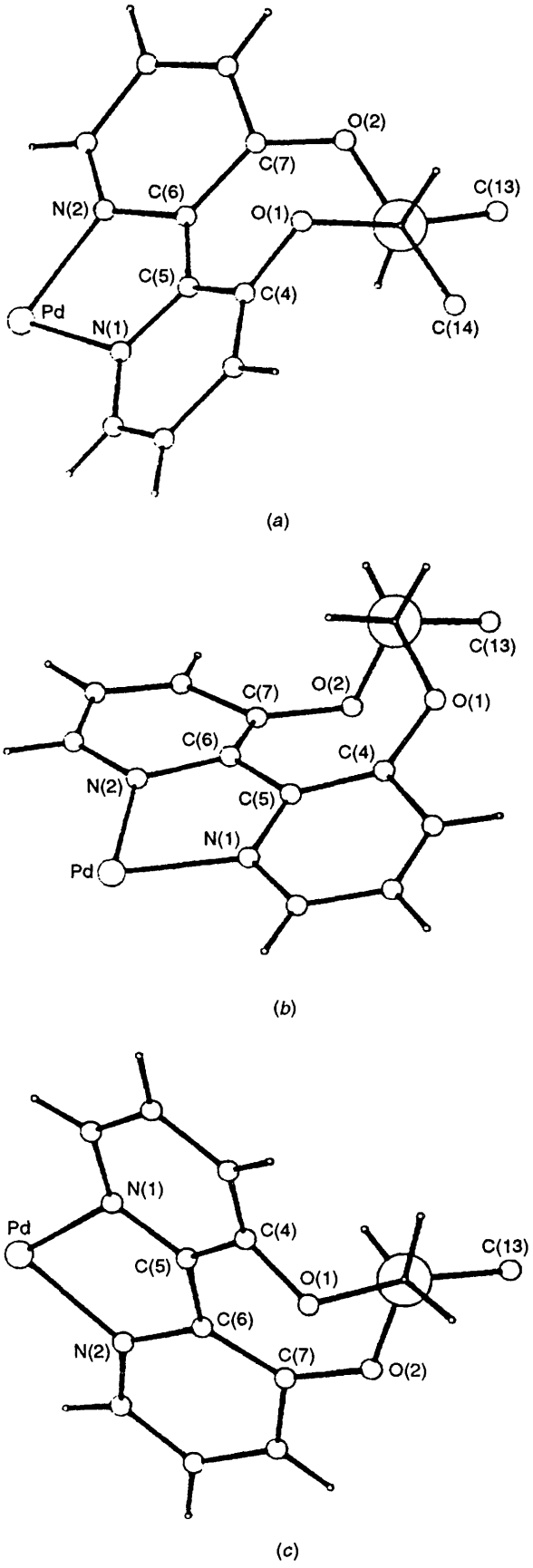

Fig. 6 Conformations of L^1 in complex **1** (*a*), L^2 in molecule A of **2** (*b*) and in molecule B of **2** (*c*), all viewed along the C(11)–C(12) bond

Conclusion

The catalytic results evidence that the monochelated trifluoracetatopalladium(II) complexes with achiral or chiral nitrogen-

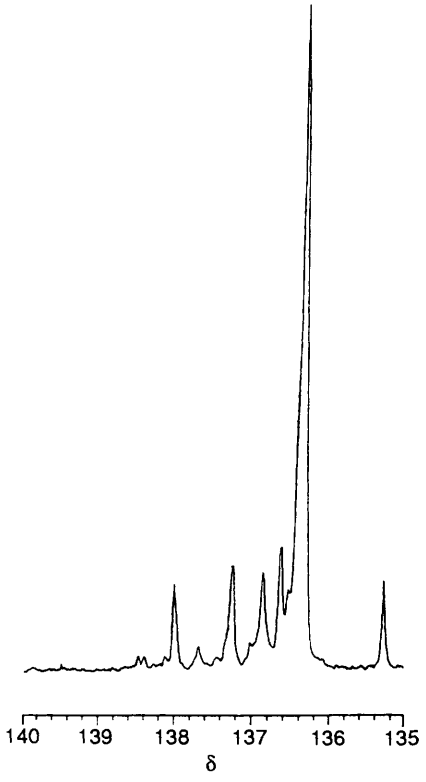

Fig. 7 The ^{13}C NMR spectrum of the CO–styrene copolymer in the region due to the *ipso*-carbon atom

donor chelating ligands are very good catalyst precursors for CO–styrene copolymerisation or dicarbonylation under mild reaction conditions. When the new atropisomeric compounds are employed a low asymmetric induction is observed; the prevailing stereochemistry of the copolymer remains, however, syndiotactic. Enantioface discrimination for styrene by the systems investigated is not sufficiently effective. This might be related to the large distance of the centre(s) of chirality of the ligands from the metal and to the loss of most of the atropisomerism of the ligands due to their almost planar conformation upon co-ordination at the palladium.

Acknowledgements

Financial support from Ministero dell'Università e della Ricerca Scientifica e Tecnologica (MURST 60%; Rome) is gratefully acknowledged.

References

1 E. Drent, J. A. M. van Broekhoven and M. J. Doyle, *J. Organomet. Chem.*, 1991, **417**, 235; E. Drent, J. A. M. van Broekhoven, M. J. Doyle and P. K. Wong, in *Ziegler Catalysts*, eds. G. Fink, R. Mühlhaupt and H. H. Brintzinger, Springer, Berlin, Heidelberg, 1995, p. 482.
2 A. Sen, *Chem. Technol.*, January 1986, 48; *Acc. Chem. Res.*, 1993, **26**, 303.
3 A. Sommazzi, F. Garbassi, G. Mestroni and B. Milani, *Eur. Pat.*, 93 200 331.2, 1993.
4 G. P. Belov, E. G. Chepaikin, A. P. Bezruchenko and V. I. Smirnov, *Polym. Sci. (Engl. Transl.)*, 1993, **35**, 1585.
5 A. X. Zhao and J. C. W. Chien, *J. Polym. Sci., Part A: Polym. Chem.*, 1992, **30**, 2735.
6 W. Keim, H. Maas and S. Mecking, *Z. Naturforsch., Teil B*, 1995, **50**, 430.
7 V. L. K. Valli and H. Alper, *J. Polym. Sci., Part A: Polym. Chem.*, 1995, **33**, 1715.
8 F. Benetollo, R. Bertani, G. Bombieri and L. Toniolo, *Inorg. Chim. Acta*, 1995, **233**, 5.
9 N. Alperwicz, *Chem. Week*, 25th January, 1995, 22; D. Medema and A. Noordam, *Chem. Magazine*, 1995, 127.
10 B. Milani, E. Alessio, G. Mestroni, A. Sommazzi, F. Garbassi, E. Zangrando, N. Bresciani-Pahor and L. Randaccio, *J. Chem. Soc., Dalton Trans.*, 1994, 1903.
11 M. Brookhart, F. C. Rix, J. M. De Simone and J. C. Barborak, *J. Am. Chem. Soc.*, 1992, **114**, 5894.
12 S. Bronco, G. Consiglio, S. Di Benedetto, M. Fehr, F. Spindler and A. Togni, *Helv. Chim. Acta*, 1995, **78**, 883; S. Bronco, G. Consiglio, A. Batistini and U. W. Suter, *Macromolecules*, 1994, **27**, 4436; Z. Jiang and A. Sen, *J. Am. Chem. Soc.*, 1995, **117**, 4455; F. Y. Xu, A. X. Zhao and J. C. W. Chien, *Makromol. Chem.*, 1993, **194**, 2579.
13 P. Corradini, C. De Rosa, A. Panunzi, G. Petrucci and P. Pino, *Chimia*, 1990, **44**, 52; C. De Rosa and P. Corradini, *Eur. Polym. J.*, 1993, **29**, 163; M. Trifuoggi, C. De Rosa, F. Auriemma, P. Corradini and S. Bruckner, *Macromolecules*, 1994, **27**, 3553.
14 M. Brookhart, M. I. Wagner, G. G. A. Balavoine and H. A. Haddou, *J. Am. Chem. Soc.*, 1994, **116**, 3641.
15 V. Busico, P. Corradini, L. Landriani and M. Trifuoggi, *Makromol. Chem., Rapid Commun.*, 1993, **14**, 261.
16 S. Bartolini, C. Carfagna and A. Musco, *Macromol. Rapid Commun.*, 1995, **16**, 9.
17 M. Barsacchi, G. Consiglio, L. Medici, G. Petrucci and U. W. Suter, *Angew. Chem., Int. Ed. Engl.*, 1991, **30**, 989.
18 M. Barsacchi, A. Batistini, G. Consiglio and U. W. Suter, *Macromolecules*, 1992, **25**, 3604.
19 P. Pino and R. Mühlhaupt, *Angew. Chem., Int. Ed. Engl.*, 1980, **19**, 857.
20 R. P. Thummel, F. Lefoulon and R. Mahadevan, *J. Org. Chem.*, 1985, **50**, 3824.
21 C. Botteghi, A. Schionato and O. De Luchi, *Synth. Commun.*, 1991, **21**, 1819.
22 M. D. Fryzuk and B. Bosnich, *J. Am. Chem. Soc.*, 1977, **99**, 6262; 1978, **100**, 5491.
23 C. K. Johnson, ORTEP, Report ORNL-5138, Oak Ridge National Laboratory, Oak Ridge, TN, 1976.
24 H. D. Flack, *Acta Cystallogr., Sect. A*, 1983, **39**, 876.
25 *International Tables for X-Ray Crystallography*, Kynoch Press, Birmingham, 1994, vol. 4.
26 B. A. Frenz, Enraf-Nonius Structure Determination Package, B. A. Frenz and Associates, College Station, TX and Enraf-Nonius, Delft, 1980.
27 G. M. Sheldrick, SHELXL 93, Program for the Refinement of Crystal Structures, University of Göttingen, 1993.
28 M. F. Semmelhack, P. Helquist, L. D. Jones, L. Keller, L. Mendelson, L. Spelts Ryano, J. Gorzynski Smith and R. D. Stauffer, *J. Am. Chem. Soc.*, 1981, **103**, 6460.
29 R. S. Cahn, C. Ingold and V. Prelog, *Angew. Chem., Int. Ed. Engl.*, 1966, **5**, 385.
30 G. B. Deacon and R. J. Phillips, *Coord. Chem. Rev.*, 1980, **33**, 227.
31 A. R. Siedle, R. A. Newmark, A. A. Kruger and L. H. Pignolet, *Inorg. Chem.*, 1981, **20**, 3399; G. M. Kaptei, jun., D. M. Grove, G. van Koten, W. J. J. Smeets and A. L. Spek, *Inorg. Chim. Acta*, 1993, **207**, 131.
32 C. Pisano, S. C. A. Nefkens and G. Consiglio, *Organometallics*, 1992, **11**, 1975.

Received 28*th July* 1995; *Paper* 5/05045F